EUROPEAN ORGANIZATION FOR NUCLEAR RESEARCH

CERN–EP/99–62

28 April 1999

Measurements of the Trilinear Gauge Boson Couplings WWV $(V \equiv \gamma, Z)$ in e^+e^- Collisions at 183 GeV

DELPHI Collaboration

Abstract

Measurements of the trilinear gauge boson couplings $WW\gamma$ and WWZ are presented from data taken by DELPHI in 1997 at an energy of 183 GeV. From a study of the reactions $e^+e^- \rightarrow \mathrm{W^+W^-}$, $e^+e^- \rightarrow We\nu$ and $e^+e^- \rightarrow \nu\nu\gamma$, values are obtained for Δg_1^Z and $\Delta\kappa_\gamma$, the differences of the WWZ charge coupling and of the $WW\gamma$ dipole couplings from their Standard Model values, and for λ_γ, the $WW\gamma$ quadrupole coupling. The observations are consistent with the predictions of the Standard Model.

(Accepted by Physics Letters B)

P.Abreu[21], W.Adam[50], T.Adye[36], P.Adzic[11], I.Ajinenko[42], Z.Albrecht[17], T.Alderweireld[2], G.D.Alekseev[16], R.Alemany[49], T.Allmendinger[17], P.P.Allport[22], S.Almehed[24], U.Amaldi[9], N.Amapane[45], S.Amato[47], E.G.Anassontzis[3], P.Andersson[44], A.Andreazza[9], S.Andringa[21], P.Antilogus[25], W-D.Apel[17], Y.Arnoud[9], B.Åsman[44], J-E.Augustin[25], A.Augustinus[9], P.Baillon[9], P.Bambade[19], F.Barao[21], G.Barbiellini[46], R.Barbier[25], D.Y.Bardin[16], G.Barker[17], A.Baroncelli[38], M.Battaglia[15], M.Baubillier[23], K-H.Becks[52], M.Begalli[6], A.Behrmann[52], P.Beilliere[8], Yu.Belokopytov[9,53], N.C.Benekos[31], A.C.Benvenuti[5], C.Berat[14], M.Berggren[25], D.Bertini[25], D.Bertrand[2], M.Besancon[39], M.Bigi[45], M.S.Bilenky[16], M-A.Bizouard[19], D.Bloch[10], H.M.Blom[30], M.Bonesini[27], W.Bonivento[27], M.Boonekamp[39], P.S.L.Booth[22], A.W.Borgland[4], G.Borisov[19], C.Bosio[41], O.Botner[48], E.Boudinov[30], B.Bouquet[19], C.Bourdarios[19], T.J.V.Bowcock[22], I.Boyko[16], I.Bozovic[11], M.Bozzo[13], P.Branchini[38], T.Brenke[52], R.A.Brenner[48], P.Bruckman[18], J-M.Brunet[8], L.Bugge[32], T.Buran[32], T.Burgsmueller[52], B.Buschbeck[50], P.Buschmann[52], S.Cabrera[49], M.Caccia[27], M.Calvi[27], T.Camporesi[9], V.Canale[37], F.Carena[9], L.Carroll[22], C.Caso[13], M.V.Castillo Gimenez[49], A.Cattai[9], F.R.Cavallo[5], V.Chabaud[9], Ph.Charpentier[9], L.Chaussard[25], P.Checchia[35], G.A.Chelkov[16], R.Chierici[45], P.Chliapnikov[42], P.Chochula[7], V.Chorowicz[25], J.Chudoba[29], K.Cieslik[18], P.Collins[9], R.Contri[13], E.Cortina[49], G.Cosme[19], F.Cossutti[9], J-H.Cowell[22], H.B.Crawley[1], D.Crennell[36], S.Crepe[14], G.Crosetti[13], J.Cuevas Maestro[33], S.Czellar[15], M.Davenport[9], W.Da Silva[23], A.Deghorain[2], G.Della Ricca[46], P.Delpierre[26], N.Demaria[9], A.De Angelis[9], W.De Boer[17], C.De Clercq[2], B.De Lotto[46], A.De Min[35], L.De Paula[47], H.Dijkstra[9], L.Di Ciaccio[37,9], J.Dolbeau[8], K.Doroba[51], M.Dracos[10], J.Drees[52], M.Dris[31], A.Duperrin[25], J-D.Durand[9], G.Eigen[4], T.Ekelof[48], G.Ekspong[44], M.Ellert[48], M.Elsing[9], J-P.Engel[10], B.Erzen[43], M.Espirito Santo[21], E.Falk[24], G.Fanourakis[11], D.Fassouliotis[11], J.Fayot[23], M.Feindt[17], P.Ferrari[27], A.Ferrer[49], E.Ferrer-Ribas[19], F.Ferro[13], S.Fichet[23], A.Firestone[1], U.Flagmeyer[52], H.Foeth[9], E.Fokitis[31], F.Fontanelli[13], B.Franek[36], A.G.Frodesen[4], R.Fruhwirth[50], F.Fulda-Quenzer[19], J.Fuster[49], A.Galloni[22], D.Gamba[45], S.Gamblin[19], M.Gandelman[47], C.Garcia[49], C.Gaspar[9], M.Gaspar[47], U.Gasparini[35], Ph.Gavillet[9], E.N.Gazis[31], D.Gele[10], L.Gerdyukov[42], N.Ghodbane[25], I.Gil[49], F.Glege[52], R.Gokieli[9,51], B.Golob[43], G.Gomez-Ceballos[40], P.Goncalves[21], I.Gonzalez Caballero[40], G.Gopal[36], L.Gorn[1,54], M.Gorski[51], Yu.Gouz[42], V.Gracco[13], J.Grahl[1], E.Graziani[38], C.Green[22], H-J.Grimm[17], P.Gris[39], G.Grosdidier[19], K.Grzelak[51], M.Gunther[48], J.Guy[36], F.Hahn[9], S.Hahn[52], S.Haider[9], A.Hallgren[48], K.Hamacher[52], J.Hansen[32], F.J.Harris[34], V.Hedberg[24], S.Heising[17], J.J.Hernandez[49], P.Herquet[2], H.Herr[9], T.L.Hessing[34], J.-M.Heuser[52], E.Higon[49], S-O.Holmgren[44], P.J.Holt[34], S.Hoorelbeke[2], M.Houlden[22], J.Hrubec[50], K.Huet[2], G.J.Hughes[22], K.Hultqvist[44], J.N.Jackson[22], R.Jacobsson[9], P.Jalocha[9], R.Janik[7], Ch.Jarlskog[24], G.Jarlskog[24], P.Jarry[39], B.Jean-Marie[19], E.K.Johansson[44], P.Jonsson[25], C.Joram[9], P.Juillot[10], F.Kapusta[23], K.Karafasoulis[11], S.Katsanevas[25], E.C.Katsoufis[31], R.Keranen[17], B.P.Kersevan[43], B.A.Khomenko[16], N.N.Khovanski[16], A.Kiiskinen[15], B.King[22], A.Kinvig[22], N.J.Kjaer[30], O.Klapp[52], H.Klein[9], P.Kluit[30], P.Kokkinias[11], M.Koratzinos[9], V.Kostioukhine[42], C.Kourkoumelis[3], O.Kouznetsov[39], M.Krammer[50], E.Kriznic[43], J.Krstic[11], Z.Krumstein[16], P.Kubinec[7], J.Kurowska[51], K.Kurvinen[15], J.W.Lamsa[1], D.W.Lane[1], P.Langefeld[52], V.Lapin[42], J-P.Laugier[39], R.Lauhakangas[15], G.Leder[50], F.Ledroit[14], V.Lefebure[2], L.Leinonen[44], A.Leisos[11], R.Leitner[29], J.Lemonne[2], G.Lenzen[52], V.Lepeltier[19], T.Lesiak[18], M.Lethuillier[39], J.Libby[34], D.Liko[9], A.Lipniacka[44], I.Lippi[35], B.Loerstad[24], J.G.Loken[34], J.H.Lopes[47], J.M.Lopez[40], R.Lopez-Fernandez[14], D.Loukas[11], P.Lutz[39], L.Lyons[34], J.MacNaughton[50], J.R.Mahon[6], A.Maio[21], A.Malek[52], T.G.M.Malmgren[44], S.Maltezos[31], V.Malychev[16], F.Mandl[50], J.Marco[40], R.Marco[40], B.Marechal[47], M.Margoni[35], J-C.Marin[9], C.Mariotti[9], A.Markou[11], C.Martinez-Rivero[19], F.Martinez-Vidal[49], S.Marti i Garcia[9], J.Masik[12], N.Mastroyiannopoulos[11], F.Matorras[40], C.Matteuzzi[27], G.Matthiae[37], F.Mazzucato[35], M.Mazzucato[35], M.Mc Cubbin[22], R.Mc Kay[1], R.Mc Nulty[22], G.Mc Pherson[22], C.Meroni[27], W.T.Meyer[1], A.Miagkov[42], E.Migliore[45], L.Mirabito[25], W.A.Mitaroff[50], U.Mjoernmark[24], T.Moa[44], M.Moch[17], R.Moeller[28], K.Moenig[9], M.R.Monge[13], X.Moreau[23], P.Morettini[13], G.Morton[34], U.Mueller[52], K.Muenich[52], M.Mulders[30], C.Mulet-Marquis[14], R.Muresan[24], W.J.Murray[36], B.Muryn[14,18], G.Myatt[34], T.Myklebust[32], F.Naraghi[14], M.Nassiakou[11], F.L.Navarria[5], S.Navas[49], K.Nawrocki[51], P.Negri[27], S.Nemecek[12], N.Neufeld[9], N.Neumeister[50], R.Nicolaidou[39], B.S.Nielsen[28], M.Nikolenko[10,16], V.Nomokonov[15], A.Normand[22], A.Nygren[24], V.Obraztsov[42], A.G.Olshevski[16], A.Onofre[21], R.Orava[15], G.Orazi[10], K.Osterberg[15], A.Ouraou[39], M.Paganoni[27], S.Paiano[5], R.Pain[23], R.Paiva[21], J.Palacios[34], H.Palka[18], Th.D.Papadopoulou[31,9], K.Papageorgiou[11], L.Pape[9], C.Parkes[9], F.Parodi[13], U.Parzefall[22], A.Passeri[38], O.Passon[52], M.Pegoraro[35], L.Peralta[21], A.Perrotta[5], C.Petridou[46], A.Petrolini[13], H.T.Phillips[36], F.Pierre[39], M.Pimenta[21], E.Piotto[27], T.Podobnik[43], M.E.Pol[6], G.Polok[18], P.Poropat[46], V.Pozdniakov[16], P.Privitera[37], N.Pukhaeva[16], A.Pullia[27], D.Radojicic[34], S.Ragazzi[27], H.Rahmani[31], P.N.Ratoff[20], A.L.Read[32], P.Rebecchi[9], N.G.Redaelli[27], M.Regler[50], D.Reid[30], R.Reinhardt[52], P.B.Renton[34], L.K.Resvanis[3], F.Richard[19], J.Ridky[12], G.Rinaudo[45], O.Rohne[32], A.Romero[45], P.Ronchese[35], E.I.Rosenberg[1], P.Rosinsky[7], P.Roudeau[19], T.Rovelli[5], Ch.Royon[39], V.Ruhlmann-Kleider[39], A.Ruiz[40], H.Saarikko[15], Y.Sacquin[39], A.Sadovsky[16], G.Sajot[14], J.Salt[49], D.Sampsonidis[11], M.Sannino[13], H.Schneider[17], Ph.Schwemling[23], B.Schwering[52], U.Schwickerath[17], M.A.E.Schyns[52], F.Scuri[46], P.Seager[20], Y.Sedykh[16], A.M.Segar[34], R.Sekulin[36], R.C.Shellard[6], A.Sheridan[22], M.Siebel[52], L.Simard[39], F.Simonetto[35], A.N.Sisakian[16], G.Smadja[25], N.Smirnov[42], O.Smirnova[24], G.R.Smith[36], O.Solovianov[42], A.Sopczak[17], R.Sosnowski[51], T.Spassov[21], E.Spiriti[38], P.Sponholz[52], S.Squarcia[13], C.Stanescu[38], S.Stanic[43], K.Stevenson[34], A.Stocchi[19], J.Strauss[50], R.Strub[10], B.Stugu[4], M.Szczekowski[51], M.Szeptycka[51], T.Tabarelli[27], F.Tegenfeldt[48], F.Terranova[27], J.Thomas[34], J.Timmermans[30], N.Tinti[5], L.G.Tkatchev[16],

S.Todorova[10], A.Tomaradze[2], B.Tome[21], A.Tonazzo[9], L.Tortora[38], G.Transtromer[24], D.Treille[9], G.Tristram[8], M.Trochimczuk[51], C.Troncon[27], A.Tsirou[9], M-L.Turluer[39], I.A.Tyapkin[16], S.Tzamarias[11], O.Ullaland[9], V.Uvarov[42], G.Valenti[5], E.Vallazza[46], G.W.Van Apeldoorn[30], P.Van Dam[30], W.K.Van Doninck[2], J.Van Eldik[30], A.Van Lysebetten[2], N.Van Remortel[2], I.Van Vulpen[30], N.Vassilopoulos[34], G.Vegni[27], L.Ventura[35], W.Venus[36,9], F.Verbeure[2], M.Verlato[35], L.S.Vertogradov[16], V.Verzi[37], D.Vilanova[39], L.Vitale[46], E.Vlasov[42], A.S.Vodopyanov[16], C.Vollmer[17], G.Voulgaris[3], V.Vrba[12], H.Wahlen[52], C.Walck[44], C.Weiser[17], D.Wicke[52], J.H.Wickens[2], G.R.Wilkinson[9], M.Winter[10], M.Witek[18], G.Wolf[9], J.Yi[1], O.Yushchenko[42], A.Zalewska[18], P.Zalewski[51], D.Zavrtanik[43], E.Zevgolatakos[11], N.I.Zimin[16,24], G.C.Zucchelli[44], G.Zumerle[35]

[1]Department of Physics and Astronomy, Iowa State University, Ames IA 50011-3160, USA
[2]Physics Department, Univ. Instelling Antwerpen, Universiteitsplein 1, BE-2610 Wilrijk, Belgium
and IIHE, ULB-VUB, Pleinlaan 2, BE-1050 Brussels, Belgium
and Faculté des Sciences, Univ. de l'Etat Mons, Av. Maistriau 19, BE-7000 Mons, Belgium
[3]Physics Laboratory, University of Athens, Solonos Str. 104, GR-10680 Athens, Greece
[4]Department of Physics, University of Bergen, Allégaten 55, NO-5007 Bergen, Norway
[5]Dipartimento di Fisica, Università di Bologna and INFN, Via Irnerio 46, IT-40126 Bologna, Italy
[6]Centro Brasileiro de Pesquisas Físicas, rua Xavier Sigaud 150, BR-22290 Rio de Janeiro, Brazil
and Depto. de Física, Pont. Univ. Católica, C.P. 38071 BR-22453 Rio de Janeiro, Brazil
and Inst. de Física, Univ. Estadual do Rio de Janeiro, rua São Francisco Xavier 524, Rio de Janeiro, Brazil
[7]Comenius University, Faculty of Mathematics and Physics, Mlynska Dolina, SK-84215 Bratislava, Slovakia
[8]Collège de France, Lab. de Physique Corpusculaire, IN2P3-CNRS, FR-75231 Paris Cedex 05, France
[9]CERN, CH-1211 Geneva 23, Switzerland
[10]Institut de Recherches Subatomiques, IN2P3 - CNRS/ULP - BP20, FR-67037 Strasbourg Cedex, France
[11]Institute of Nuclear Physics, N.C.S.R. Demokritos, P.O. Box 60228, GR-15310 Athens, Greece
[12]FZU, Inst. of Phys. of the C.A.S. High Energy Physics Division, Na Slovance 2, CZ-180 40, Praha 8, Czech Republic
[13]Dipartimento di Fisica, Università di Genova and INFN, Via Dodecaneso 33, IT-16146 Genova, Italy
[14]Institut des Sciences Nucléaires, IN2P3-CNRS, Université de Grenoble 1, FR-38026 Grenoble Cedex, France
[15]Helsinki Institute of Physics, HIP, P.O. Box 9, FI-00014 Helsinki, Finland
[16]Joint Institute for Nuclear Research, Dubna, Head Post Office, P.O. Box 79, RU-101 000 Moscow, Russian Federation
[17]Institut für Experimentelle Kernphysik, Universität Karlsruhe, Postfach 6980, DE-76128 Karlsruhe, Germany
[18]Institute of Nuclear Physics and University of Mining and Metalurgy, Ul. Kawiory 26a, PL-30055 Krakow, Poland
[19]Université de Paris-Sud, Lab. de l'Accélérateur Linéaire, IN2P3-CNRS, Bât. 200, FR-91405 Orsay Cedex, France
[20]School of Physics and Chemistry, University of Lancaster, Lancaster LA1 4YB, UK
[21]LIP, IST, FCUL - Av. Elias Garcia, 14-1^o, PT-1000 Lisboa Codex, Portugal
[22]Department of Physics, University of Liverpool, P.O. Box 147, Liverpool L69 3BX, UK
[23]LPNHE, IN2P3-CNRS, Univ. Paris VI et VII, Tour 33 (RdC), 4 place Jussieu, FR-75252 Paris Cedex 05, France
[24]Department of Physics, University of Lund, Sölvegatan 14, SE-223 63 Lund, Sweden
[25]Université Claude Bernard de Lyon, IPNL, IN2P3-CNRS, FR-69622 Villeurbanne Cedex, France
[26]Univ. d'Aix - Marseille II - CPP, IN2P3-CNRS, FR-13288 Marseille Cedex 09, France
[27]Dipartimento di Fisica, Università di Milano and INFN, Via Celoria 16, IT-20133 Milan, Italy
[28]Niels Bohr Institute, Blegdamsvej 17, DK-2100 Copenhagen Ø, Denmark
[29]NC, Nuclear Centre of MFF, Charles University, Areal MFF, V Holesovickach 2, CZ-180 00, Praha 8, Czech Republic
[30]NIKHEF, Postbus 41882, NL-1009 DB Amsterdam, The Netherlands
[31]National Technical University, Physics Department, Zografou Campus, GR-15773 Athens, Greece
[32]Physics Department, University of Oslo, Blindern, NO-1000 Oslo 3, Norway
[33]Dpto. Fisica, Univ. Oviedo, Avda. Calvo Sotelo s/n, ES-33007 Oviedo, Spain
[34]Department of Physics, University of Oxford, Keble Road, Oxford OX1 3RH, UK
[35]Dipartimento di Fisica, Università di Padova and INFN, Via Marzolo 8, IT-35131 Padua, Italy
[36]Rutherford Appleton Laboratory, Chilton, Didcot OX11 OQX, UK
[37]Dipartimento di Fisica, Università di Roma II and INFN, Tor Vergata, IT-00173 Rome, Italy
[38]Dipartimento di Fisica, Università di Roma III and INFN, Via della Vasca Navale 84, IT-00146 Rome, Italy
[39]DAPNIA/Service de Physique des Particules, CEA-Saclay, FR-91191 Gif-sur-Yvette Cedex, France
[40]Instituto de Fisica de Cantabria (CSIC-UC), Avda. los Castros s/n, ES-39006 Santander, Spain
[41]Dipartimento di Fisica, Università degli Studi di Roma La Sapienza, Piazzale Aldo Moro 2, IT-00185 Rome, Italy
[42]Inst. for High Energy Physics, Serpukov P.O. Box 35, Protvino, (Moscow Region), Russian Federation
[43]J. Stefan Institute, Jamova 39, SI-1000 Ljubljana, Slovenia and Laboratory for Astroparticle Physics,
Nova Gorica Polytechnic, Kostanjeviska 16a, SI-5000 Nova Gorica, Slovenia,
and Department of Physics, University of Ljubljana, SI-1000 Ljubljana, Slovenia
[44]Fysikum, Stockholm University, Box 6730, SE-113 85 Stockholm, Sweden
[45]Dipartimento di Fisica Sperimentale, Università di Torino and INFN, Via P. Giuria 1, IT-10125 Turin, Italy
[46]Dipartimento di Fisica, Università di Trieste and INFN, Via A. Valerio 2, IT-34127 Trieste, Italy
and Istituto di Fisica, Università di Udine, IT-33100 Udine, Italy
[47]Univ. Federal do Rio de Janeiro, C.P. 68528 Cidade Univ., Ilha do Fundão BR-21945-970 Rio de Janeiro, Brazil
[48]Department of Radiation Sciences, University of Uppsala, P.O. Box 535, SE-751 21 Uppsala, Sweden
[49]IFIC, Valencia-CSIC, and D.F.A.M.N., U. de Valencia, Avda. Dr. Moliner 50, ES-46100 Burjassot (Valencia), Spain
[50]Institut für Hochenergiephysik, Österr. Akad. d. Wissensch., Nikolsdorfergasse 18, AT-1050 Vienna, Austria
[51]Inst. Nuclear Studies and University of Warsaw, Ul. Hoza 69, PL-00681 Warsaw, Poland
[52]Fachbereich Physik, University of Wuppertal, Postfach 100 127, DE-42097 Wuppertal, Germany
[53]On leave of absence from IHEP Serpukhov
[54]Now at University of Florida

1 Introduction

This study of the trilinear gauge boson couplings at the WWV vertex, with $V \equiv \gamma, Z$, uses data from the reactions $e^+e^- \to \mathrm{W^+W^-}$, $e^+e^- \to We\nu$ and $e^+e^- \to \nu\nu\gamma$ taken by the DELPHI detector at LEP in 1997 at a centre-of-mass energy of 183 GeV. Results are given for three coupling parameters: Δg_1^Z, the difference between the value of the overall WWZ coupling strength and its Standard Model prediction; $\Delta\kappa_\gamma$, the difference between the value of the dipole coupling, κ_γ, and its Standard Model value; and λ_γ, the $WW\gamma$ quadrupole coupling parameter.

In the evaluation of these parameters, a model has been assumed [1] in which contributions to the effective WWV Lagrangian from operators describing possible new physics beyond the Standard Model are restricted to those which are CP-conserving, are of lowest dimension (≤ 6), satisfy $SU(2) \times U(1)$ invariance and have not been excluded by previous measurements. This leads to possible contributions from three operators, $\mathcal{L}_{W\phi}$, $\mathcal{L}_{B\phi}$ and $\mathcal{L}_W$, and hence to relations between the permitted values of the $WW\gamma$ and WWZ couplings: $\Delta\kappa_Z = \Delta g_1^Z - \frac{s_w^2}{c_w^2}\Delta\kappa_\gamma$, $\lambda_Z = \lambda_\gamma$, where s_w and c_w are the sine and cosine of the electroweak mixing angle. The parameters we determine are related to possible contributions $\alpha_{W\phi}$, $\alpha_{B\phi}$ and α_W from the three operators given above by: $\Delta g_1^Z = \alpha_{W\phi}/c_w^2$, $\Delta\kappa_\gamma = \alpha_{W\phi} + \alpha_{B\phi}$, and $\lambda_\gamma = \alpha_W$. In previous DELPHI studies of trilinear gauge couplings [2,3], limits have been expressed in terms of these α parameters.

The WWV coupling arises in WW production through the diagrams involving s-channel exchange of Z or γ, shown in figure 1a. We study this reaction in the final state $jj\ell\nu$ (where j represents a quark jet) arising from the decay of one W into quarks and the other into leptons, and in the final state $jjjj$, where both Ws decay into quarks.

In single W production, the dominant amplitude involving a trilinear gauge coupling arises from the radiation of a virtual photon from the incident electron or positron, interacting with a virtual W radiated from the other incident particle (figure 1b). This process, involving a $WW\gamma$ coupling, contributes significantly in the kinematic region where a final state electron or positron is emitted at small angle to the beam and is thus likely to remain undetected in the beam pipe. The decay modes of the W give rise to two final states: that with two jets and missing energy (jjX), and that containing only a single lepton coming from the interaction point and no other track in the detector (ℓX). Other processes, involving both $WW\gamma$ and WWZ couplings, also contribute to the events selected in this kinematic region. They include those shown in figure 1a, when one W decays into $e\nu$, and the Z radiation process shown in figure 1b, which combine coherently with the contribution from the virtual photon radiation diagram. Nonetheless, the jjX and ℓX final states remain more sensitive to $WW\gamma$ than to WWZ couplings, and have been shown to be particularly sensitive to the coupling $\Delta\kappa_\gamma$ [4].

The trilinear $WW\gamma$ vertex also occurs in the reaction $e^+e^- \to \nu\nu\gamma$ in the diagram in which the incoming electron and positron each radiate a virtual W at an $e\nu W$ vertex and these two fuse to produce an outgoing photon (figure 1c). In this process, which leads to a final state, γX, consisting of a single detected photon, the $WW\gamma$ coupling is studied completely independently of the WWZ coupling, as no WWZ vertex is involved. In the Standard Model, the dominant mechanism for production of this final state is via the reaction $e^+e^- \to Z\gamma$, with the photon produced by initial state radiation and with the Z decaying into $\nu\bar{\nu}$. This reaction could also proceed via anomalous couplings at a $ZV\gamma$ vertex, a possibility which we study in a separate paper [5]; here we assume that all $ZV\gamma$ couplings are equal to zero, as predicted by the Standard Model.

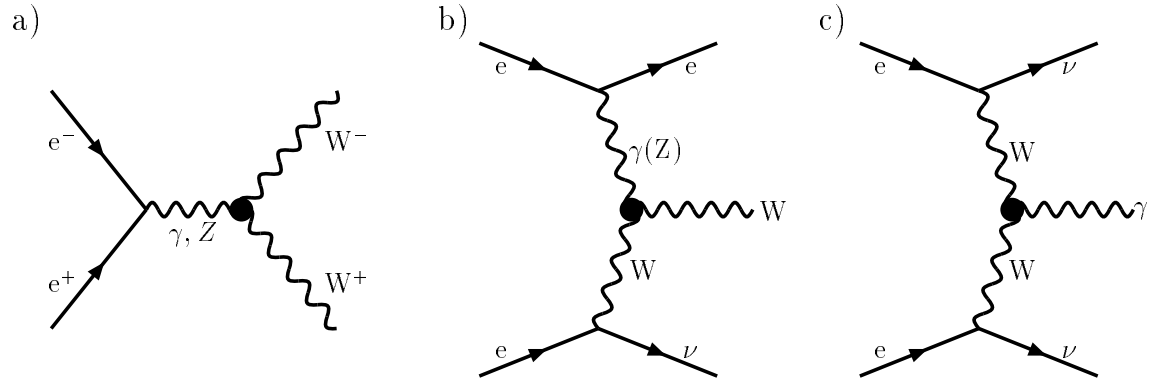

Figure 1: Diagrams with trilinear gauge boson couplings contributing to the processes studied in this paper: a) $e^+e^- \rightarrow$ W^+W^-, b) $e^+e^- \rightarrow We\nu$, c) $e^+e^- \rightarrow \nu\nu\gamma$.

The next section of this paper describes the selection of events from the data and the simulation of the various channels involved in the analysis, and section 3 describes the methods used in the determination of coupling parameters. In section 4 the results from different channels are presented and combined to give overall values for the coupling parameters. A summary is given in section 5.

2 Event selection and simulation

In 1997 DELPHI recorded a total integrated luminosity of 53 pb^{-1} at an average centre-of-mass energy of 182.7 GeV. We describe here the main features of the selection of events in the final state topologies $jj\ell\nu$, $jjjj$, jjX, ℓX and γX defined in the previous section. A detailed description of the DELPHI detector and its performance may be found in [6], which includes descriptions of the main components of the detector used in this study, namely, the trigger system, the luminosity monitor, the tracking system in the barrel and forward regions, the muon detectors, the electromagnetic calorimeters and the hermeticity counters. The definition of the criteria imposed for track selection and lepton identification are the same as those used in [7], where a description of the luminosity measurement is also given.

Selection of events in the $jj\ell\nu$ topology:

Events in the $jj\ell\nu$ topology are characterized by two hadronic jets, a lepton and missing momentum taken by the neutrino. The lepton may be an electron or muon (coming either from W decay or from the cascade decay $W \rightarrow \tau ... \rightarrow \ell ...$) or, in the case of τ decays, it might give rise to a low multiplicity jet. The major backgrounds come from $q\bar{q}(\gamma)$ production and from four-fermion final states containing two quarks and two leptons of the same flavour.

Events with several hadrons were selected by requiring 5 or more charged particles and total energy of charged particles recorded in the detector exceeding 15% of the centre-of-mass energy. In the selection of $jj\mu\nu$ and $jje\nu$ events, the candidate lepton was assumed to be the most energetic charged particle in the event, while for $jj\tau\nu$ events the lepton candidates were constructed by looking for an isolated e or μ or a low multiplicity jet.

All particles except that corresponding to the candidate lepton were forced into two jets using the LUCLUS algorithm [8]. To remove $\gamma\gamma$ interactions and poorly reconstructed events each quark jet was required to have no less than 4 particles, at least one being charged, and the invariant mass of the two jets was required to exceed 30 GeV/c^2. Furthermore, events were required to have missing momentum above 10 GeV/c and no detected isolated photon with energy above 40 GeV.

Events with a candidate muon in the final state were accepted if the momentum of the candidate exceeded 25 GeV/c (or 5 GeV/c for τ candidates decaying into muons) and if the isolation angle of the candidate (defined as the angle between the muon and the nearest particle with momentum above 1 GeV/c) exceeded a value between 8° and 20°, depending on the quality of the muon identification. Non-isolated particles which were tagged as muons were also considered as candidates if the missing momentum of the event exceeded 20 GeV/c and if the polar angle of the missing momentum, $\theta_{p_{miss}}$, satisfied $|\cos\theta_{p_{miss}}| < 0.95$.

The selection of events with an electron candidate in the final state followed a similar procedure: charged particles with energy deposition in the electromagnetic calorimeters of at least 20 GeV were accepted as candidates. (For tau candidates decaying into electrons, the energy deposition was required to exceed 5 GeV and to match the momentum within ±20%). The component of the missing momentum transverse to the beam axis was required to be greater than 10 GeV/c and the angle between the candidate and the missing momentum to exceed 90°. The isolation angle of the candidate with respect to the nearest charged particle of momentum greater than 1 GeV/c was required to exceed 5° for electrons observed in the barrel region of the detector, or 10° for electrons in the forward region.

In order to increase the efficiency of the selection, events where the candidate was not identified as a lepton were also considered. Kinematic requirements in this case were tighter, accepting only events satisfying $|\cos\theta_{p_{miss}}| < 0.95$ (or < 0.87 for events where the lepton was an electron candidate). In addition, events were required to satisfy the condition $\sqrt{s'} < \sqrt{s} - 5$ GeV, where $\sqrt{s'}$ is an estimate of the effective collision energy in the (background) $q\bar{q}(\gamma)$ final state after initial state radiation [9].

Four-fermion backgrounds ($q\bar{q}\ell\ell$) were reduced by applying an additional cut to events in which a second lepton of the same flavour and with charge opposite to that of the candidate was found. Such events were rejected if the second lepton had momentum above 5 GeV/c and isolation angle with respect to all other particles except the candidate greater than 15°.

Events were selected as $jj\tau\nu$ candidates with a τ decaying into hadrons if both the missing energy and the transverse energy exceeded 40 GeV and if at least 3 jets were reconstructed using LUCLUS with $d_{join} = 3$ GeV/c. The tau candidate jet was required to have measured multiplicity below 6, only one charged particle, total momentum above 10 GeV/c and to be isolated from other jets by more than 25°. In addition, in order to reduce the fully hadronic WW background, the event was rejected if it had four or more jets reconstructed with $d_{join} = 10$ GeV/c.

A 3-constraint kinematic fit [7] was then performed on candidate e and μ events, imposing energy and momentum conservation and the nominal W mass on both Ws. For candidate τ events, a 2-constraint fit was performed, in which the τ momentum was left unconstrained, while its direction was taken to be that of its detected decay products.

The efficiency for the selection of $jj\ell\nu$ events was evaluated using fully simulated events to be (89.0±0.4)%, (68.5±0.5)% and (33.8±0.6)% for $jj\mu\nu$, $jje\nu$ and $jj\tau\nu$ events respectively. Using data corresponding to an integrated luminosity of 50.2 pb^{-1}, taken

when all essential components of the detector were working, a sample of 108 muon, 90 electron and 45 tau events was selected, including an estimated background contamination of 18.3 $\pm$ 1.1 events of which 72% came from the $q\bar{q}(\gamma)$ final state, 18% from Ze^+e^- and 10% from ZZ and $Z\gamma^*$ production.

Selection of events in the $jjjj$ topology:

In the selection of events in the fully hadronic topology, all detected particles were first clustered into jets using LUCLUS with $d_{join} = 6.5$ GeV/c. Events were accepted if they had at least four jets, with at least four particles per jet. Background from $Z\gamma$ events was suppressed by imposing the condition $\sqrt{s'} > 130$ GeV. Events were then forced into a 4-jet configuration and a 5-constraint fit performed, requiring conservation of four-momentum and the two reconstructed W masses to be equal. The fit was applied to all three possible pairings of the four jets into two Ws. Fits with reconstructed W mass outside the range $74 < m_W^{rec} < 88$ GeV/c^2 were rejected and, of the remaining fits, the one with minimum χ^2 was accepted. Then, in order to suppress the dominant background, which arises from the $q\bar{q}\gamma$ final state, the condition $D > 0.0045$ rad·GeV^{-1} was imposed, with $D = \frac{E_{min}}{E_{max}}\theta_{min}/(E_{max} - E_{min})$; E_{min} and E_{max} are the minimum and maximum energies of the fitted jets and θ_{min} is the minimum interjet angle. The use of the D-variable is illustrated in reference [7].

The efficiency of the selection procedure was evaluated from fully simulated events to be (76.8 ± 0.3)%. A total of 383 events was selected from data corresponding to an integrated luminosity of 53.0 pb^{-1}, containing estimated background contributions of 77.9 ± 3.7 events from $q\bar{q}\gamma$ production and 3.3 ± 0.2 events from the $jj\ell\nu$ final state. The method used in the data to assign the reconstructed jets to W pairs was applied to a sample of simulated events generated with only the three doubly resonant diagrams for WW production present in the production amplitude; in this model the efficiency of the procedure was estimated to be about 75%.

An additional problem in the analysis of the $jjjj$ state is to distinguish the pair of jets constituting the W^+ decay products from that from the W^-. This ambiguity can be partly resolved by computing jet charges from the momentum-weighted charge of each particle belonging to the jet, $Q_{jet} = \sum_i q_i |p|_i^{0.5} / \sum_i |p|_i^{0.5}$ (where the exponent is chosen empirically), and defining the $W^\pm$ charges, Q_{W^+} and Q_{W^-}, as the sums of the charges of the two daughter jets. Following the method of [10], the distribution of the difference $\Delta Q = Q_{W^-} - Q_{W^+}$ was then used to construct an estimator $P(\Delta Q)$ of the probability that the pair with the more negative value of Q_W is a W^-. An estimate of the efficiency of this procedure was made by flagging all correctly associated jet pairs reconstructed from simulated events with $\Delta Q < 0$ as W^- and comparing with the generated information: a value of 76% was obtained.

Selection of events in the jjX topology:

Events were selected as candidates for the jjX topology, in which an electron is presumed lost in the beam pipe and a neutrino is assumed to be produced, if they had at least 6 charged particles, total visible energy in the event less than 110 GeV, total measured transverse momentum greater than 15 GeV/c, invariant mass of detected particles exceeding 45 GeV/c^2, and a total energy deposition in the very forward electromagnetic calorimeter [6] less than 65 GeV. All detected particles were then clustered into jets using LUCLUS with $d_{join} = 5.5$ GeV/c. Events were accepted if they had exactly two jets, with at least two charged particles in each jet.

Events from the WW final state, with one W decaying leptonically, were suppressed by rejecting events with identified final state leptons (e or μ) of energy exceeding 12 GeV, or with an isolated particle (at more than 10° from the nearest charged particle) of energy greater than 10 GeV and with energy deposition in the electromagnetic calorimeters exceeding 5 GeV. Further rejection of the $jj\tau\nu$ final state was achieved by requiring the mass of the more energetic jet to be less than 20 GeV/c^2 and the mass of the other jet to be less than 15 GeV/c^2.

In order to suppress the contribution from the $q\bar{q}\gamma$ final state, events were rejected if the two jets were collinear to within 20° or if the angle between the planes containing each jet direction and the beam was less than 20°. In addition, events were rejected if there was a signal in the hermeticity detectors within 30° of the direction of the missing momentum. Finally, a kinematic fit to the reaction $e^+e^-\to jj\gamma$ was made to the event, assuming the presence of an unseen additional photon, and requiring 4-momentum conservation. Events were rejected if the direction of the reconstructed photon lay within 25° of the beam direction.

In the determination of coupling parameters from these data, the number of observed events was compared with the predicted number. The selection efficiency was evaluated using fully simulated events defined in a region of the four-fermion phase space somewhat wider than that used in the selection of events from the data, and was found to be constant with respect to the couplings within the accuracy of the estimation, and equal to (55±2)% for $q\bar{q}e\nu$ production after application of the selection procedure described above. From the integrated luminosity of 53.0 pb^{-1} 17 events were selected. For Standard Model values of the couplings a total of 19.2 events was expected, comprising 6.0 ± 0.35 $q\bar{q}e\nu$ events in the jjX topology, 1.1 ± 0.05 events from $q\bar{q}e\nu$ with the electron or positron emitted into the detector acceptance, 6.3 ± 0.2 events from $q\bar{q}\tau\nu$, 1.7 ± 0.07 events from $q\bar{q}\mu\nu$, 0.7 ± 0.05 events from $q\bar{q}\nu\bar{\nu}$, 3.4 ± 0.15 events from $q\bar{q}\gamma$ production, and negligible contributions from other sources. All the processes contributing to the selected sample except the $q\bar{q}\gamma$ production include diagrams with trilinear gauge couplings, and this was taken into account in the subsequent analysis.

Selection of events in the ℓX topology:

The selection of events in the ℓX topology required events with only one charged particle which was clearly identified as a muon or electron according to criteria defined in [7]. The normal track selections were tightened in order to reject cosmic ray background: the track was required to pass within 1 mm of the interaction point in the xy plane (perpendicular to the beam) and within 4 cm in z. Lepton candidates were also required to have momentum below 75 GeV/c, with transverse component above 20 GeV/c. Events were rejected if there was an energy deposition of more than 3 GeV in the barrel or forward electromagnetic calorimeters which was not associated with the charged particle track, or if the hermeticity detectors showed a signal which, when projected on to the xy plane, was at an angle of more than 120° to the candidate track.

Using these criteria, one electron event and 7 muon events were selected from the data, while totals of 1.85 and 3.47 events were expected for Standard Model values of the couplings in the two channels, respectively. In the eX sample, 1.60 ± 0.2 events were expected from $\ell\nu\ell'\nu'$ production, coming mainly from the $e_I\nu e\nu$ final state (where e_I denotes an undetected electron), for which a selection efficiency of (50 ± 5)% was estimated in the kinematic region used in the calculation. The sample in the μX topology was estimated to contain 2.52 ± 0.3 $\ell\nu\ell'\nu'$ events, mainly from the $e_I\nu\mu\nu$ final state, which was selected with an efficiency of (74 ± 5)%. The samples also contain smaller

contributions from other $\ell\nu\ell'\nu'$ final states, including those involving τ production. The eX sample was estimated to contain a background contribution of 0.25 ± 0.09 events from $e^+e^-\gamma$ production, and backgrounds of 0.34 ± 0.12 and 0.61 ± 0.35 events were estimated in the muon channel from $\mu\mu\gamma$ and $e^+e^-\mu^+\mu^-$ production, respectively. Other backgrounds, including that due to cosmic ray muons, were estimated to be negligible. The comparison of the predicted and observed total numbers of events was made in the same manner as for the jjX topology, described above.

Selection of events in the γX topology:

The production of the single photon final state, γX, via a $WW\gamma$ vertex proceeds through the fusion diagram shown in figure 1c, while the dominant process giving rise to this final state, $e^+e^-\to Z\gamma$, with $Z\to\nu\bar{\nu}$, involves bremsstrahlung diagrams. The sensitivity of the γX final states to anomalous $WW\gamma$ couplings is therefore greatest when the photon is emitted at high polar angle and with high energy. Events were selected if they had a single shower in the barrel electromagnetic calorimeter, with $45^\circ < \theta_\gamma < 135^\circ$ and $E_\gamma > 50$ GeV, where θ_γ and E_γ are the polar angle and energy, respectively, of the reconstructed photon. It was also required that no electromagnetic showers were present in the forward electromagnetic calorimeters, and a second shower in the barrel calorimeter was accepted only if it was within 20° of the first one. Cosmic ray events were suppressed by requiring that any signal in the hadronic calorimeter was in the same angular region as the signal in the electromagnetic calorimeter, and that the electromagnetic shower should point towards the beam collision point [11]. Using these criteria, 39 events were selected from data corresponding to an integrated luminosity of 50.2 pb^{-1}. In the region with $E_\gamma > 50$ GeV, trigger and identification efficiencies of $(90 \pm 3)\%$ and $(78 \pm 2)\%$, respectively, were estimated, giving an overall selection efficiency of $(70 \pm 4)\%$. Negligible background was estimated.

Event simulation:

Various Monte Carlo models were used in the calculation of cross-sections as a function of coupling parameters in the different final states analysed. In the study of the $jj\ell\nu$ and $jjjj$ channels, the four-fermion generators EXCALIBUR [12] and ERATO [13] were used, the $We\nu$ final states used calculations based on the program DELTGC [14], cross-checked with GRC4F [15], and DELTGC and NUNUGPV [16] were used to calculate expected signals in the γX topology. The EXCALIBUR and GRC4F models were interfaced to the JETSET hadronization model [8], tuned to Z data [17], and to the full DELPHI simulation program [6]. In addition, in the analysis of the $jj\ell\nu$ final state, a fast simulation of the DELPHI detector was used. Cross-checks were made to ensure that the fast and full simulations agreed in the distributions of the kinematic variables used in the analysis. The study of backgrounds due to $q\bar{q}(\gamma)$ production was made using fully simulated events from the PYTHIA model [18], while EXCALIBUR was used to study the $qq\nu\nu$ contribution to the jjX topology and KORALZ [19] was used in the calculation of backgrounds in the ℓX final state. PYTHIA and EXCALIBUR were used in the simulation of events from ZZ production. Two-photon backgrounds were studied using the generators of Berends, Daverveldt and Kleiss [20] and with the TWOGAM generator [21].

3 Methods used in the determination of the couplings

Data in the $jj\ell\nu$ and $jjjj$ channels were analysed using methods based on that of Optimal Observables [22]. The methods exploit the fact that the differential cross-section, $d\sigma/d\vec{V}$, where $\vec{V}$ represents the phase space variables, is quadratic in the trilinear gauge coupling parameters:

$$\frac{d\sigma(\vec{V},\vec{\lambda})}{d\vec{V}} = c_0(\vec{V}) + \sum_i c_1^i(\vec{V})\cdot\lambda_i + \sum_{i,j} c_2^{ij}(\vec{V})\cdot\lambda_i\cdot\lambda_j\,,$$

where the sums in i,j are over the set $\vec{\lambda} = \{\lambda_1,\ldots,\lambda_n\}$ of parameters under consideration. The parameters c_0, c_1^i and c_2^{ij} in this expression can be evaluated at any phase space point (for instance, using the calculations of ERATO) from the squared transition matrix element for production of the relevant four-fermion final state for given values of the coupling parameters.

The analysis of data in the $jj\ell\nu$ final state followed the method of reference [23], in which the probability distribution function of the reconstructed phase space $\vec{\Omega}$ (expressed as the reconstructed four-vectors of the four final-state fermions) is expanded about a general set of coupling parameters $\vec{\lambda}_0$. Then "Modified Observables" are defined as the mean values of the quantities

$$\omega_i(\vec{\Omega},\vec{\lambda}_0) = \frac{y_1^i(\vec{\Omega},\vec{\lambda}_0)}{y_0(\vec{\Omega},\vec{\lambda}_0)}\,,$$

where $y_0(\vec{\Omega},\vec{\lambda}_0)$ and $y_1^i(\vec{\Omega},\vec{\lambda}_0)$ are, respectively, the constant and linear terms of the Taylor expansion of the probability distribution function, readily evaluated as linear combinations of the c_0, c_1^i and c_2^{ij} above. In [23], it is shown that, for values of $\vec{\lambda}$ close to the expansion point $\vec{\lambda}_0$, the ω_i defined above are essentially as effective in estimating the $\vec{\lambda}$ as an unbinned likelihood fit of the parameters to the data. The expected behaviour (n-dimensional calibration surfaces) of the means $<\omega_i(\vec{\lambda}_0)>$ were computed as a function of the couplings using samples of fully simulated events generated at a few values of the couplings and reweighted [24] to cover the desired region of parameter space. Values of $<\omega_i(\vec{\lambda}_0)>$ were evaluated from the data sample and compared to the expectation surfaces by means of a maximum likelihood fit, taking into account the limited statistics both of the experiment and of the simulated events used in the evaluation of the calibration surfaces. Since the optimal estimating efficiency of this technique is achieved only when the uncertainty on the measurement of the Modified Observable lies within the linear part of the calibration surface around the expansion point, an iterative procedure in $\vec{\lambda}_0$ was employed which was considered to converge when the fitted values of the couplings differed from the expansion values by amounts which were negligible compared with the statistical errors in the determination of the parameters.

In the analysis of the $jjjj$ final state, for which the precision expected from the present data does not require application of an iterative procedure, a somewhat simpler application of the method of Optimal Observables was used. The quantities $\omega_i(\vec{\Omega},\vec{\lambda}_0)$, expanded about Standard Model values of the parameters, $\vec{\lambda}_0 = \vec{\lambda}_{SM}$, were computed from fully simulated events, again using reweighted events generated at a few values of the couplings, and compared with the data using binned maximum likelihood fits to the

shape and absolute normalization of the distributions. The distribution of $\omega(\vec{\Omega}, \vec{\lambda}_{SM})$ for the coupling parameter Δg_1^Z is shown in figure 2 together with the expected distribution for the value of the coupling obtained from the fit, given in table 1.

In the analysis of data in the $jj\ell\nu$ and $jjjj$ channels, it is not known which jet from a W decay comes from the quark and which from the antiquark, leading to a twofold ambiguity for $jj\ell\nu$ and a fourfold ambiguity for $jjjj$. For each event in the analyses described above, the average of the contributions from each assignment was used in the construction of the likelihood function.

A second method was applied to the determination of couplings in the $jj\ell\nu$ channel. In this analysis, a binned maximum likelihood fit was made to the joint distribution in the well-measured variables $\cos\theta_W$, the W^- production angle, and $\cos\theta_\ell$, the polar angle of the produced lepton with respect to the incoming $e^\pm$ of the same sign, without application of a kinematic fit. Relaxation of the latter requirement led to a slightly larger sample of selected events: 118, 97 and 49 events in the muon, electron and tau channels, respectively. The expected distribution in the ($\cos\theta_W$, $\cos\theta_\ell$) plane for given values of the coupling parameters was calculated using ERATO together with a fast simulation of the detector response. The distributions of $\cos\theta_W$ and $\cos\theta_\ell$ for the combined leptonic sample are shown in figure 3 together with the expected distributions for the value of Δg_1^Z obtained from the fit.

Data in the single W topologies, jjX, eX and μX, were analysed using a maximum likelihood fit to the observed total numbers of events selected. The selection of events in these topologies was designed to enhance the contribution from the virtual photon radiation process of figure 1b which, as mentioned in section 1, involves only the $WW\gamma$ coupling and is particularly sensitivity to $\Delta\kappa_\gamma$. The selected data sample in each of the three topologies contains contributions from final states involving this diagram, as well as contributions from final states involving WWV couplings but not the virtual photon radiation process. There are also contributions from backgrounds without any dependence on trilinear gauge couplings. The evaluation of the expected signal in each topology took all these contributions and their dependences on the coupling parameters into account. Calculations of the expected cross-sections, selected as described in section 2, showed that, for Standard Model values of the couplings, the μX channel is expected to provide the greatest precision in the determination of $\Delta\kappa_\gamma$, with the data from the jjX and eX channels providing upper limits on $\Delta\kappa_\gamma$ poorer than that from μX by factors of about two and four, respectively.

Data in the γX topology were analysed using a maximum likelihood fit to the binned distribution of the photon energy spectrum. The energy spectrum of the data is shown in figure 4 together with the expected distribution for the value of $\Delta\kappa_\gamma$ obtained from the fit.

The analysis procedures described above have been tested using samples of fully simulated data corresponding to the same integrated luminosity as the real data and have been shown to reproduce the values of the couplings used in the generation of the events to within the expected statistical precision.

4 Results on WWV couplings

The results and one standard deviation errors obtained for the couplings Δg_1^Z, $\Delta\kappa_\gamma$ and λ_γ from the data in each of the final states and using the methods discussed above are shown in table 1. In the fit to each coupling parameter, the values of the other parameters were held at zero, their Standard Model value. In some cases, the assignment of confidence

intervals is complicated by the fact that the quadratic dependence of the cross-section with coupling parameters can give rise to a log-likelihood distribution with two minima. This is the case in the determination of $\Delta\kappa_\gamma$ in the ($\cos\theta_W$, $\cos\theta_\ell$) analysis, where the upper 68% confidence limit is not well determined, and in the fit to λ_γ in the single W topologies, where we quote only the 95% confidence interval. In the determination of coupling parameters from the γX topology, in which both total cross-section data and the shape of the photon energy spectrum were used, the main part of the precision comes from the cross-section which, after correction for losses in the selection procedure, was determined to be $(1.09 \pm 0.17(stat.) \pm 0.05(syst.))$ pb in the accepted kinematic region.

The log-likelihood distributions from all topologies (using the Modified Observables method for $jj\ell\nu$) were combined to give the values of the coupling parameters, their one standard deviation uncertainties and the 95% confidence limits shown in table 2. Agreement between the data and the predictions from the fits (shown, for example, in figures 2, 3 and 4), is good. The results of fits in which two parameters were allowed to vary are shown in figure 5. In all cases, the results are consistent with the Standard Model prediction of zero for the couplings we determine.

Topology	Δg_1^Z	$\Delta\kappa_\gamma$	λ_γ
$jj\ell\nu$ (Modified Observables)	$-0.04^{+0.16}_{-0.15} \pm 0.02$	$0.12^{+0.66}_{-0.52} \pm 0.12$	$-0.15^{+0.19}_{-0.17} \pm 0.03$
$jj\ell\nu$ ($\cos\theta_W$, $\cos\theta_\ell$)	$-0.10^{+0.17}_{-0.15} \pm 0.02$	$-0.05^{+1.49}_{-0.46} \pm 0.19$	$-0.19^{+0.18}_{-0.16} \pm 0.02$
$jjjj$	$-0.02^{+0.29}_{-0.24} \pm 0.10$	$0.17^{+1.24}_{-0.63} \pm 0.25$	$-0.09^{+0.34}_{-0.25} \pm 0.15$
$jjX + \ell X$	$0.10^{+0.94}_{-1.05} \pm 0.11$	$0.26^{+0.38}_{-0.48} \pm 0.15$	$-1.13 < \lambda_\gamma < 1.14$ (95% C.L.)
γX	—	$0.02^{+1.25}_{-1.22} \pm 0.06$	$0.06^{+1.53}_{-1.53} \pm 0.10$

Table 1: Fitted values of WWV couplings from DELPHI data at 183 GeV using the methods described in the text. The first errors given for each value are the one standard deviation statistical uncertainties; the second is the systematic error. For the fit to λ_γ in the single W topologies the 95% confidence limits are shown (see text). A 1 standard deviation systematic error of 0.10 was estimated in this case. In the fits to each coupling parameter, the other two couplings were set to their Standard Model value.

Coupling parameter	Value $\pm 1\sigma$	95% confidence interval
Δg_1^Z	$-0.04^{+0.14}_{-0.12}$	$-0.28 < \Delta g_1^Z < 0.24$
$\Delta\kappa_\gamma$	$0.19^{+0.32}_{-0.34}$	$-0.46 < \Delta\kappa_\gamma < 0.84$
λ_γ	$-0.15^{+0.19}_{-0.15}$	$-0.44 < \lambda_\gamma < 0.24$

Table 2: Values of WWV couplings combining DELPHI data at 183 GeV from all final states listed in table 1. In the $jj\ell\nu$ topology, the results obtained with the method of Modified Observables (see text) were used in the combination. The second column shows the value of each coupling corresponding to the minimum of the combined negative log-likelihood distribution and its 1 standard deviation errors. The third column shows the 95% confidence intervals on the parameter values. Both the statistical errors and the independent systematic errors are included.

Various effects contribute to the systematic errors included in the results in tables 1 and 2. These uncertainties are small compared to the statistical precision attained with the present data. Effects common to more than one of the selected final states include

the uncertainties in the W mass, taken to be ± 100 MeV/c^2, in the integrated luminosity ($\pm 1\%$) and in the beam energy (± 50 MeV), and the theoretical uncertainty in the calculation of the WW cross-section (taken to be $\pm 2\%$ [1]). These were evaluated for each final state studied, and combined with weights derived from the statistical errors in the determination of each coupling parameter to give overall estimates of ± 0.01 in Δg_1^Z, ± 0.01 in $\Delta\kappa_\gamma$ and ± 0.02 in λ_γ. These common errors are in addition to the independent systematic uncertainties included in the confidence intervals shown in table 2. The systematic effects specific to each final state include those arising from the statistical errors in the calculation of signal and background cross-sections due to the finite statistics of the simulated events used, and from the effect of the event reconstruction procedure on the energies assigned to jets and leptons. In addition, possible effects due to the choice of the jet hadronization model used in the analysis were estimated by comparing results from samples simulated with JETSET, ARIADNE [25] and HERWIG [26]. In the $jjjj$ final state, the effect of the uncertainty in the computation of jet charges used to distinguish W^+ from W^- was considered, and possible colour reconnection effects were studied by comparing samples generated with and without type II´ colour reconnection, as defined in [27].

5 Conclusions

Values for the trilinear gauge couplings WWV have been derived from an analysis of DELPHI data at 183 GeV. The following results have been obtained:

$$\Delta g_1^Z = -0.04^{+0.14}_{-0.12}\ , \quad \Delta\kappa_\gamma = \ 0.19^{+0.32}_{-0.34}\ , \quad \lambda_\gamma \ = -0.15^{+0.19}_{-0.15}\ .$$

These results and the results from the 2-parameter fits shown in figure 5 are consistent with Standard Model predictions. The precisions achieved represent an improvement by a factor $\sim 2-3$ over those obtained in the previous DELPHI analysis of data at 161 and 172 GeV.

Acknowledgements

We are greatly indebted to our technical collaborators, to the members of the CERN-SL Division for the excellent performance of the LEP collider, and to the funding agencies for their support in building and operating the DELPHI detector.
We acknowledge in particular the support of
Austrian Federal Ministry of Science and Traffics, GZ 616.364/2-III/2a/98,
FNRS–FWO, Belgium,
FINEP, CNPq, CAPES, FUJB and FAPERJ, Brazil,
Czech Ministry of Industry and Trade, GA CR 202/96/0450 and GA AVCR A1010521,
Danish Natural Research Council,
Commission of the European Communities (DG XII),
Direction des Sciences de la Matière, CEA, France,
Bundesministerium für Bildung, Wissenschaft, Forschung und Technologie, Germany,
General Secretariat for Research and Technology, Greece,
National Science Foundation (NWO) and Foundation for Research on Matter (FOM), The Netherlands,
Norwegian Research Council,
State Committee for Scientific Research, Poland, 2P03B06015, 2P03B03311 and SPUB/P03/178/98,
JNICT–Junta Nacional de Investigação Científica e Tecnológica, Portugal,
Vedecka grantova agentura MS SR, Slovakia, Nr. 95/5195/134,
Ministry of Science and Technology of the Republic of Slovenia,
CICYT, Spain, AEN96–1661 and AEN96-1681,
The Swedish Natural Science Research Council,
Particle Physics and Astronomy Research Council, UK,
Department of Energy, USA, DE–FG02–94ER40817.

References

[1] G. Gounaris, J.-L. Kneur and D. Zeppenfeld, in *Physics at LEP2*, eds. G. Altarelli, T. Sjöstrand and F. Zwirner, CERN 96-01 Vol.1, 525 (1996).

[2] DELPHI Collaboration, P. Abreu *et al.*, Phys. Lett. **B397** (1997) 158.

[3] DELPHI Collaboration, P. Abreu *et al.*, Phys. Lett. **B423** (1998) 194.

[4] see, for example, R. Tanaka, *Single W production at LEP2*, hep-ex/9811039, Proceedings of ICHEP98, Vancouver, (1998), to be published.

[5] DELPHI Collaboration, *Study of Trilinear Gauge Boson Couplings $ZZ\gamma$ and $Z\gamma\gamma$ at 183 GeV*, Abstract 329, contributed to ICHEP98, Vancouver, (1998).

[6] DELPHI Collaboration, P. Aarnio *et al.*, Nucl. Inst. Meth. **A303** (1991) 233,
DELPHI Collaboration, P. Abreu *et al.*, Nucl. Inst. Meth. **A378** (1996) 57.

[7] DELPHI Collaboration, P. Abreu *et al.*, E. Phys. J. **C2** (1998) 581.

[8] T. Sjöstrand, *PYTHIA 5.7 / JETSET 7.4*, CERN-TH.7112/93 (1993).

[9] P. Abreu *et al.*, *The Estimation of the Effective Centre of Mass Energy in q-qbar-gamma Events from DELPHI*, CERN-OPEN-98-026, hep-ex/9809008, (1998), Nucl. Inst. Meth. **A**, to be published.

[10] ALEPH Collaboration, R. Barate *et al.*, Phys. Lett. **B422** (1998) 369.

[11] DELPHI Collaboration, *Analysis of the single photon channel at LEP 2*, Abstract 206, contributed to ICHEP98, Vancouver, (1998).

[12] F.A. Berends, R. Kleiss and R. Pittau, *EXCALIBUR*, in *Physics at LEP2*, eds. G. Altarelli, T. Sjöstrand and F. Zwirner, CERN 96-01 Vol.2, 23 (1996).

[13] C.G. Papadopoulos, Comp. Phys. Comm. **101** (1997) 183.

[14] O. Yushchenko, *DELTGC: A program for four-fermion calculations*, DELPHI note DELPHI 99-4 PHYS 816 (1999).

[15] J. Fujimoto *et al., GRC4F*, in *Physics at LEP2*, eds. G. Altarelli, T. Sjöstrand and F. Zwirner, CERN 96-01 Vol.2, 23 (1996).

[16] G. Montagna *et al.* Nucl. Phys. **B452** (1995) 161.

[17] DELPHI Collaboration, P. Abreu *et al.*, Z. Phys. **C73** (1996) 11.

[18] T. Sjöstrand, *PYTHIA 5.719 / JETSET 7.4*, in *Physics at LEP2*, eds. G. Altarelli, T. Sjöstrand and F. Zwirner, CERN 96-01 Vol.2, 41 (1996).

[19] S. Jadach, B.F.L Ward and Z. W as, Comp. Phys. Comm. **79** (1994) 503.

[20] F.A. Berends, P.H. Daverveldt and R. Kleiss, Comp. Phys. Comm. **40** (1980) 271, 285 and 309.

[21] S. Nova, S. Olchevski and T. Todorov, in *Physics at LEP2*, eds. G. Altarelli, T. Sjöstrand and F. Zwirner, CERN 96-01 Vol.2, 224 (1996).

[22] M. Diehl and O. Nachtmann, Z. Phys. **C62** (1994) 397.

[23] G.K. Fanourakis, D. Fassouliotis and S.E. Tzamarias, Nucl. Inst. Meth. **A414** (1998) 399,
G.K. Fanourakis, D. Fassouliotis, A. Leisos, N. Mastroyiannopoulos and S.E. Tzamarias, *Extended Modified Observable technique for a Multi-Parametric Trilinear Gauge Coupling Estimation at LEP II*, hep-ex/9812002 (1998), Nucl. Inst. Meth. **A**, to be published.

[24] G.K. Fanourakis, D.A. Fassouliotis and S.E. Tzamarias, Nucl. Inst. Meth. **A412** (1998) 465.

[25] L. Lonnblad, Comp. Phys. Comm. **71** (1992) 15.

[26] G. Marchesini, B.R. Webber, G. Abbiendi, I.G. Knowles, M.H. Seymour and L. Stanco, Comp. Phys. Comm. **67** (1992) 465.

[27] T. Sjöstrand and V. Khoze, Z. Phys. **C62** (1994) 281.

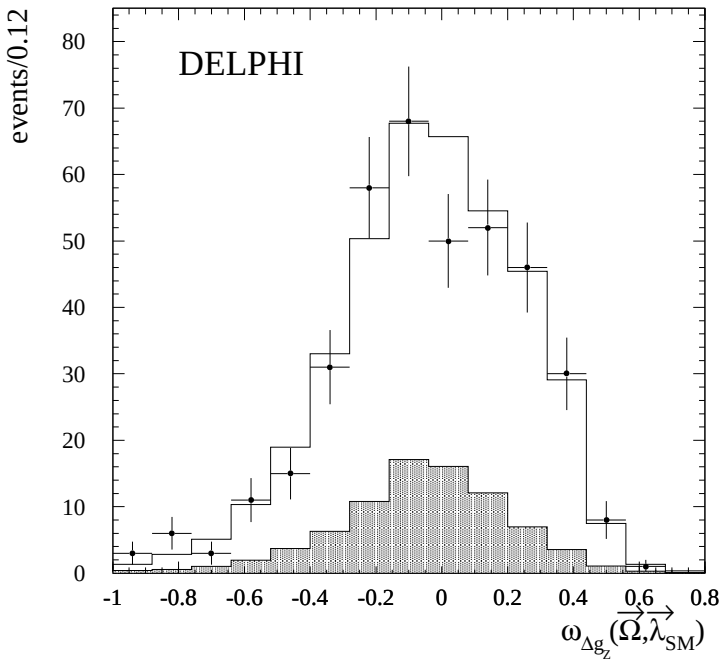

Figure 2: Distribution of the optimal variable $\omega(\vec{\Omega}, \vec{\lambda}_{SM})$ (defined in the text) for the coupling Δg_1^Z in the $jjjj$ channel at 183 GeV. The points represent the data and the histogram the expectation for the value of Δg_1^Z obtained from the fit, shown in table 1, with background contributions shaded.

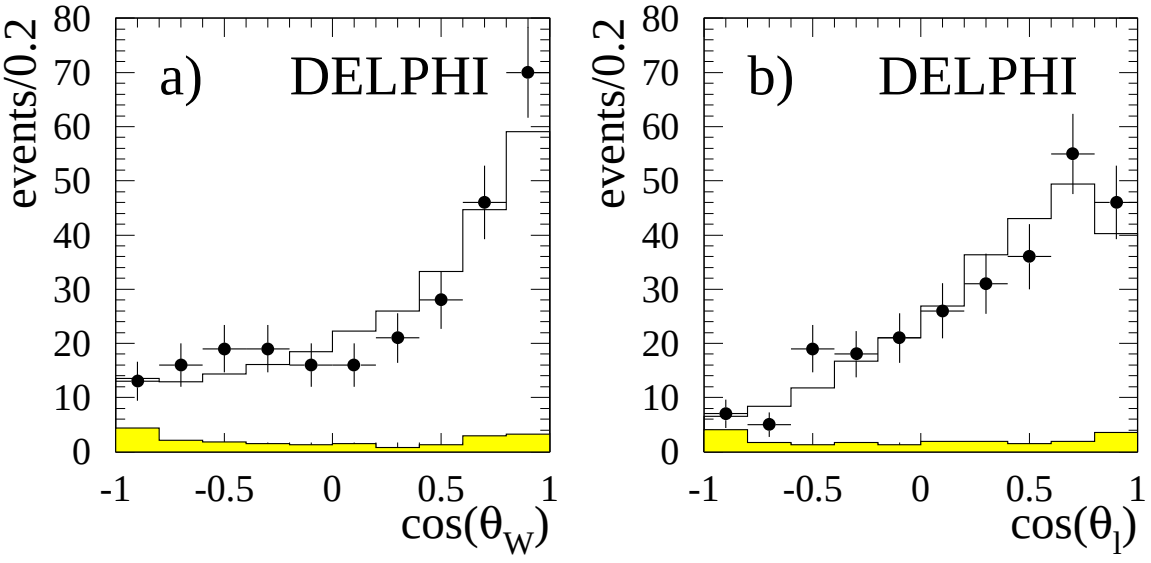

Figure 3: Distribution of a) $\cos\theta_W$ and b) $\cos\theta_\ell$ in the $jj\ell\nu$ final state at 183 GeV. The points represent the data and the histograms the expectation for the value of Δg_1^Z obtained from the fit, shown in table 1, with background contributions shaded.

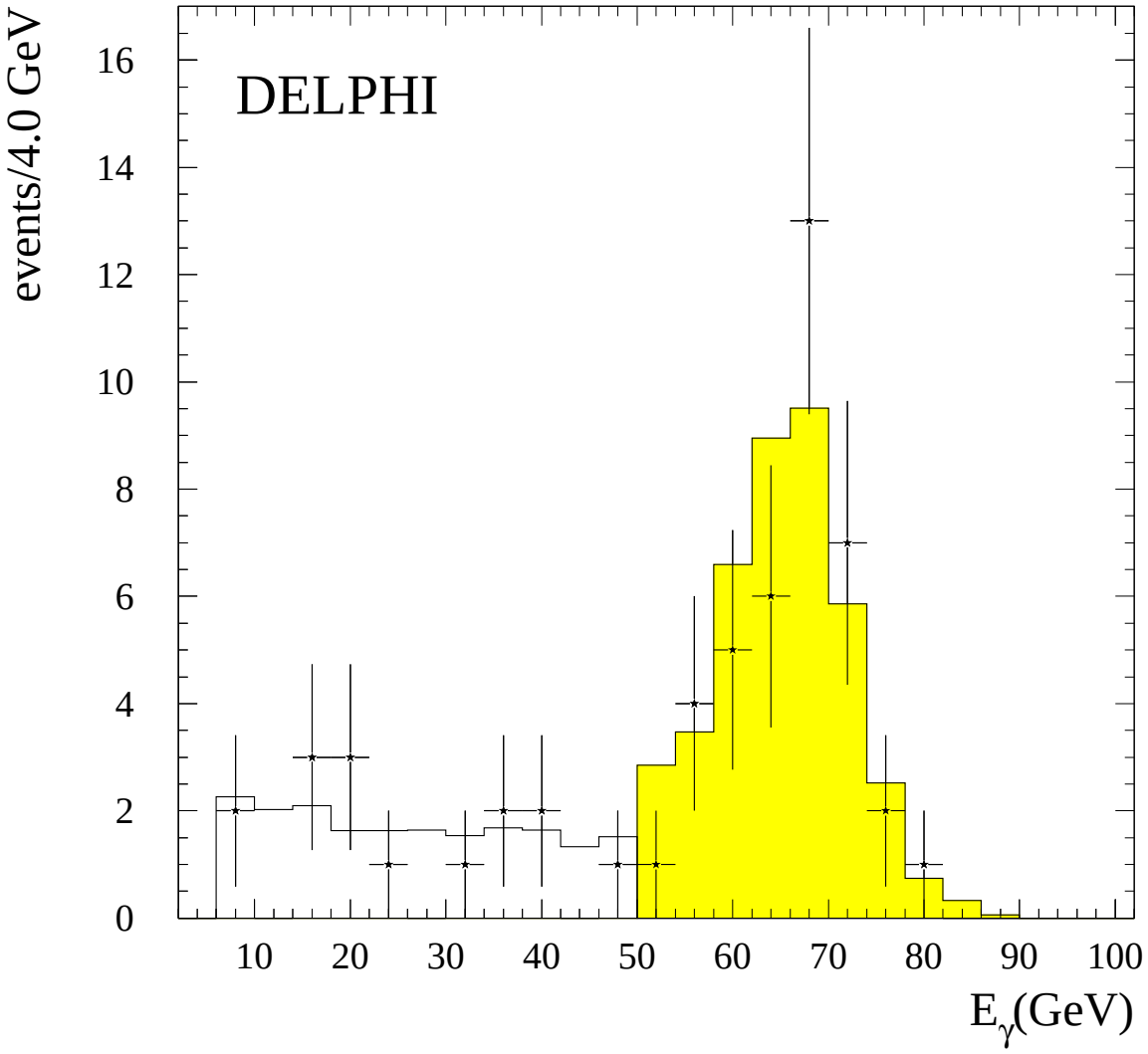

Figure 4: Photon energy spectrum of selected single photon events at 183 GeV. The crosses show the data and the histogram is the expectation for the value of $\Delta\kappa_\gamma$, shown in table 1, obtained from the fit to the distribution in the shaded region, $E_\gamma > 50$ GeV. The background contribution in the selected data sample is negligible.

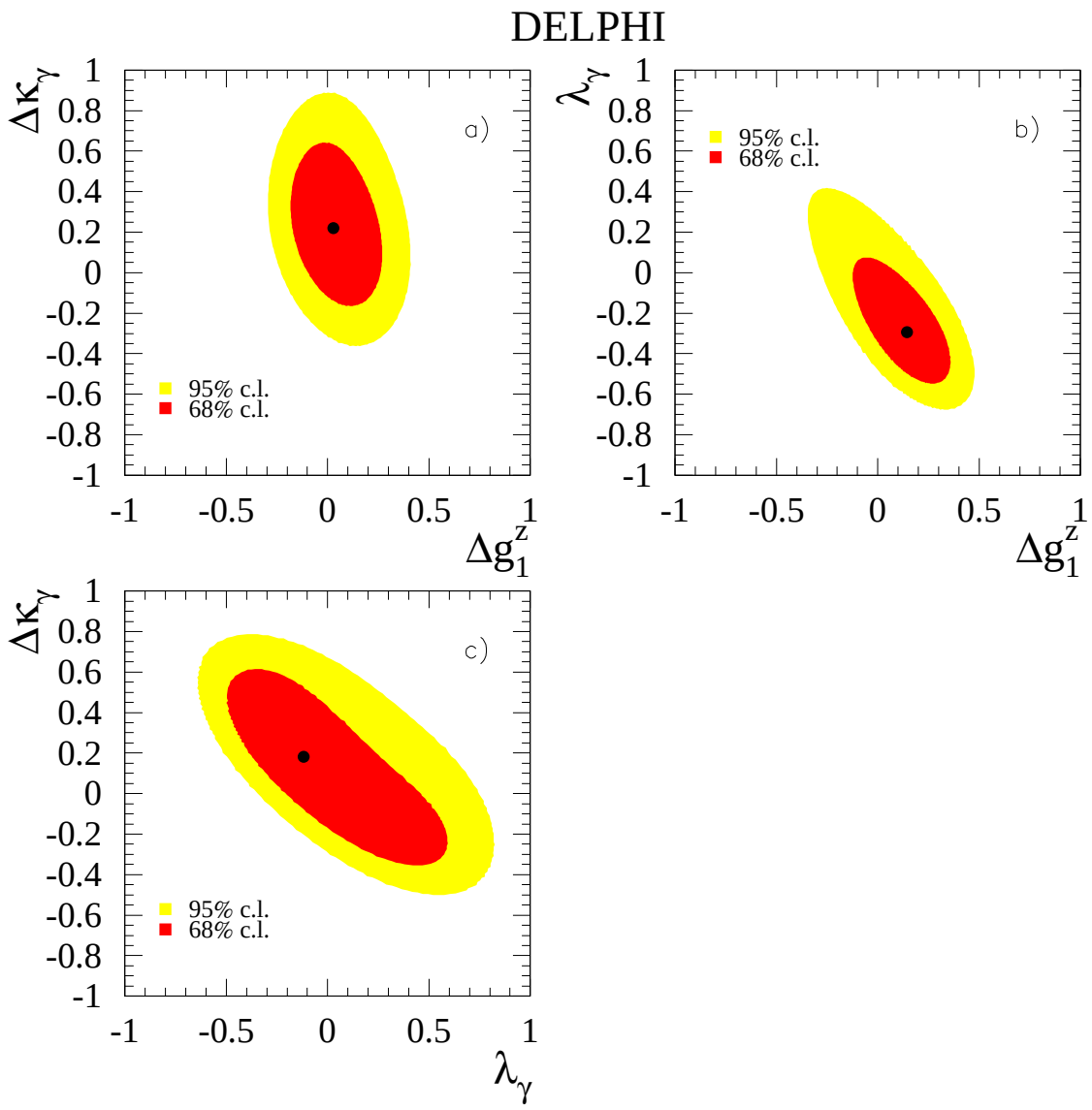

Figure 5: Results of fits in the plane of parameters a) (Δg_1^Z, $\Delta\kappa_\gamma$), b) (Δg_1^Z, λ_γ), c) (λ_γ, $\Delta\kappa_\gamma$) using DELPHI data at 183 GeV from all final states listed in table 1. In the fit to each pair of parameters, the value of the third parameter was set to its Standard Model value. The regions accepted at the 68% and 95% confidence levels are shown. The points at the centres of the accepted regions indicate the values maximizing the likelihood functions.